15 June 2000

ELSEVIER

Optics Communications 180 (2000) 377–382

OPTICS COMMUNICATIONS

www.elsevier.com/locate/optcom

Spatiotemporal solitons in inhomogeneous nonlinear media

S. Raghavan [a,*], Govind P. Agrawal [b]

[a] *Rochester Theory Center for Optical Science & Engineering, Department of Physics & Astronomy, University of Rochester, Rochester, NY 14627, USA*

[b] *The Institute of Optics, University of Rochester, Rochester, NY 14627, USA*

Received 10 February 2000; received in revised form 13 April 2000; accepted 14 April 2000

Abstract

We investigate the possibility of forming spatiotemporal solitons (optical bullets) in inhomogeneous, dispersive nonlinear media using a graded-index Kerr medium as an example. We use a variational approach to solve the multidimensional, inhomogeneous, nonlinear Schrödinger equation and show that spatiotemporal solitons can be stabilized under certain conditions. We verify their existence by means of a full numerical analysis and show that such solitons should be observable experimentally. © 2000 Published by Elsevier Science B.V. All rights reserved.

PACS: 42.65.-k; 42.65.Jx; 42.65.S; 42.65.Tg; 42.82.Dp

Optical solitons have been shown to form and propagate inside a nonlinear Kerr medium [1–3]. They are called temporal or spatial solitons depending on whether their shape remains intact in time or in one space dimension. Mathematically, wave propagation in a Kerr medium is governed by the nonlinear Schrödinger equation (NLSE), which can be solved exactly in $(1+1)$-dimensions by using the inverse scattering method [1–3]. Whether an optical soliton can be confined simultaneously in space and time is a question that has attracted considerable attention in recent years [4–15], and the term optical bullet has been coined for such a soliton. Among other applications, optical bullets are useful for all-optical digital logic [9]. Most of previous work has focused on solitons formed in a self-focusing medium exhibiting anomalous dispersion. In this paper, we consider pulse propagation in a general nonlinear, dispersive medium with special emphasis on a self-defocusing medium with normal dispersion. An example of such a medium occurs for visible or near-infrared light propagating inside a semiconductor. To counteract the beam spreading due to self-defocusing, we assume that the refractive index is spatially nonuniform as in a graded-index medium. An example of such a nonlinear medium is provided by the semiconductor-doped graded-index silica fiber.

We analyze the possibility of formation of stable spatiotemporal solitons in an inhomogeneous Kerr medium, for which the refractive index is of the form

$$n(\boldsymbol{r},\omega) = n_0(\omega) + n_1(x^2+y^2) + n_2|\boldsymbol{E}|^2, \qquad (1)$$

where the homogeneous part $n_0(\omega)$ takes into account chromatic dispersion, n_2 is the nonlinear parameter responsible for self-focusing or self-defocusing, and n_1 governs the change in refractive index in

* Corresponding author. E-mail: srirag@pas.rochester.edu

0030-4018/00/$ - see front matter
PII: S0030-4018(00)00727-6

the transverse dimensions x and y. Light is assumed to propagate along the z axis. The medium can be anti-guiding ($n_1 > 0$) or guiding ($n_1 < 0$). We consider both cases in this work to examine the interplay between self-(de)focusing of light and guiding/anti-guiding and dispersive effects of the medium.

Our analysis begins with Maxwell's equations, supplemented by Eq. (1). We introduce the envelope $A(\boldsymbol{r},t)$ of the electric field oscillating at the frequency ω_0 as

$$\boldsymbol{E}(\boldsymbol{r},t) = \tfrac{1}{2}\hat{e}A(\boldsymbol{r},t)\exp[\mathrm{i}(\beta_0 z - \omega_0 t)] + \text{c.c.} \quad (2)$$

Using a standard procedure and making the paraxial and the slowly varying envelope approximations [1,2], we obtain the following equation for $A(\boldsymbol{r},t)$:

$$\mathrm{i}\left(\frac{\partial A}{\partial z} + \beta_1\frac{\partial A}{\partial t}\right) - \frac{\beta_2}{2}\frac{\partial^2 A}{\partial t^2} + \frac{1}{2\beta_0}\left(\frac{\partial^2 A}{\partial x^2} + \frac{\partial^2 A}{\partial y^2}\right) + \frac{n_1}{k_0}(x^2+y^2)A + k_0 n_2|A|^2 A = 0, \quad (3)$$

where $\beta_0 = n_0(\omega_0)k_0$, $\beta_1 = (\mathrm{d}\beta/\mathrm{d}\omega)_{\omega=\omega_0}$, and $\beta_2 = (\mathrm{d}^2\beta/\mathrm{d}\omega^2)_{\omega=\omega_0}$, with $\beta = n_0(\omega)\omega/c$ and $k_0 = \omega_0/c$. We consider both positive and negative β_2 and n_2 to consider self-focusing and self-defocusing Kerr media with normal and anomalous group-velocity dispersion (GVD). Our goal is to investigate the interplay between dispersion, diffraction, index inhomogeneity and Kerr nonlinearity so that stable optical bullets may form.

To normalize Eq. (3), we introduce a transverse length scale $w_0 = (2k_0|n_1|\beta_0)^{-1/4}$ and scale the transverse coordinates as $(X,Y) = (x,y)/w_0$. Similarly, we introduce a longitudinal length scale using the diffraction length, $L_d = \beta_0 w_0^2$, and scale the longitudinal coordinate as $Z = z/L_d$. We also introduce a scaled local time $\tau = (t - \beta_1 z)/T_0$ where $T_0 = \sqrt{|\beta_2|L_d}$. In terms of these normalized variables, Eq. (3) takes the form

$$\mathrm{i}\frac{\partial U}{\partial Z} + \frac{1}{2}\left(\frac{\partial^2 U}{\partial X^2} + \frac{\partial^2 U}{\partial Y^2}\right) + \frac{\delta}{2}\frac{\partial^2 U}{\partial \tau^2} + \frac{s}{2}(X^2+Y^2)U + \nu|U|^2 U = 0, \quad (4)$$

where $U(X,Y,Z,\tau) = \sqrt{k_0 n_2 L_d}\,A(x,y,z,t)$, and the parameters $\delta = \text{sign}(\beta_2) = \pm 1$, $s = \text{sign}(n_1) = \pm 1$, and $\nu = \text{sign}(n_2) = \pm 1$, according as whether the medium has anomalous or normal GVD, is anti-guiding or guiding, and is self-focusing or self-defocusing respectively.

Eq. (4) is similar to the standard multidimensional NLSE [4]. The only difference is the term resulting from the inhomogeneous nature of the nonlinear medium. We also note that Eq. (4) is similar to the Gross–Pitaevskii equation that describes the dynamics of confined atomic Bose–Einstein condensates [16]. The crucial difference is that whereas the trapping potential is present in all three space dimensions for the condensate case, the trapping produced by the graded index is two-dimensional. Note also the sign associated with the τ-derivative: To confine the optical pulse temporally, GVD can be normal or anomalous.

One usually resorts to time-consuming numerical computations to obtain solutions of Eq. (4). Here we first use the variational method to obtain physical insight in terms of a few relevant parameters and then present numerical simulations that confirm the analytic predictions qualitatively. The variational method has been used successfully to address a variety of nonlinear problems [1–3]. It is easy to show that the NLSE (4) can be cast as a variational problem using the Lagrangian density

$$\mathscr{L} = \frac{\mathrm{i}}{2}\left(U\frac{\partial U^*}{\partial Z} - U^*\frac{\partial U}{\partial Z}\right) + \frac{1}{2}\left[\left|\frac{\partial U}{\partial X}\right|^2 + \left|\frac{\partial U}{\partial Y}\right|^2\right] + \frac{\delta}{2}\left|\frac{\partial U}{\partial \tau}\right|^2 - \frac{s}{2}(X^2+Y^2)|U|^2 - \frac{\nu}{2}|U|^4. \quad (5)$$

The choice of the trial function is crucial in the success of a variational method. We first observe from Eq. (4) that in the temporal dimension, the combination of normal GVD and self-defocusing can result in a 'sech'-type bright soliton in the temporal dimension. Furthermore, in the transverse spatial dimensions X and Y, graded-index wave-guiding leads to Hermite–Gauss modes such that the fundamental mode is Gaussian in shape. In the absence of such confinement, the time and space dimensions should be treated symmetrically. However, since we believe that the transverse confinement is strong, we take our trial function to be the product of a chirped 'sech' pulse and a chirped Gaussian beam such that

$$U(X,Y,Z,\tau) = \sqrt{\frac{\varepsilon\eta}{2\pi a^2}}\,\mathrm{sech}(\eta\tau) \times \exp\left[-(X^2+Y^2)/(2a^2)\right] \times \exp\left[\mathrm{i}\left(\theta\tau^2+\alpha(X^2+Y^2)+\phi\right)\right], \quad (6)$$

where U is normalized such that $\int |U|^2 \,\mathrm{d}X\mathrm{d}Y\mathrm{d}\tau = \varepsilon$ represents the constant pulse energy. The parameters η, a, θ, α, and ϕ, are allowed to vary with Z and represent, respectively, the temporal width, spatial width, temporal chirp, spatial chirp, and phase associated with the pulse.

We adopt the standard procedure and obtain the effective Lagrangian $L = \int \mathrm{d}X\mathrm{d}Y\mathrm{d}\tau\, \mathscr{L}(U,U^*)$ by integrating over X,Y, and τ. The result is given by

$$L = \varepsilon\left[\frac{\mathrm{d}\phi}{\mathrm{d}Z} + \frac{\pi^2}{12\eta^2}\frac{\mathrm{d}\theta}{\mathrm{d}Z} + a^2\frac{\mathrm{d}\alpha}{\mathrm{d}Z} + \frac{\delta\eta^2}{6} + \frac{\delta\theta^2\pi^2}{6\eta^2} + \frac{1}{2a^2}\left(1-\frac{\nu\varepsilon\eta}{6\pi}\right) + \frac{a^2}{2}(4\alpha^2 - s)\right]. \quad (7)$$

We then use the Euler–Lagrange equations and obtain the following set of equations:

$$\frac{\mathrm{d}\phi}{\mathrm{d}Z} = \frac{\eta^2}{3} + 4\alpha^2a^2 - \frac{7\varepsilon\eta}{24\pi a^2}, \quad (8a)$$

$$\frac{\mathrm{d}\eta}{\mathrm{d}Z} = -2\delta\eta\theta \equiv F(\eta,\theta,a,\alpha), \quad (8b)$$

$$\frac{\mathrm{d}\theta}{\mathrm{d}Z} = \frac{2\delta\eta^4}{\pi^2} - 2\delta\theta^2 - \frac{\nu\varepsilon\eta^3}{2\pi^3a^2} \equiv G(\eta,\theta,a,\alpha), \quad (8c)$$

$$\frac{\mathrm{d}a}{\mathrm{d}Z} = 2a\alpha \equiv I(\eta,\theta,a,\alpha), \quad (8d)$$

$$\frac{\mathrm{d}\alpha}{\mathrm{d}Z} = \frac{1}{2a^4} - 2\alpha^2 - \frac{\nu\varepsilon\eta}{12\pi a^4} + \frac{s}{2} \equiv J(\eta,\theta,a,\alpha). \quad (8e)$$

Note that whereas the phase ϕ is driven by the parameters η,a, and α, the evolution of η,θ,a, and α does not depend on ϕ. Therefore, Eq. (8a) is not considered further.

We first investigate the existence and stability of stationary states of the system described by Eqs. (8). The stationary states are found by setting the Z-derivatives to zero. There are two meaningful solutions, both of which are chirp-free ($\theta_{st} = 0$, $\alpha_{st} = 0$). One of the solutions ($\eta_{st} = 0$, $a_{st} = 1$) corresponds to a CW beam. The other solution corresponds to spatiotemporal solitons and is characterized by the following relations between the temporal and spatial widths

$$\eta_{st} = \frac{\nu\varepsilon}{4\delta\pi a_{st}^2}, \quad s = -\frac{1}{a_{st}^4}\left[1 - \frac{\nu^2\varepsilon^2}{24\pi^2\delta a_{st}^2}\right]. \quad (9)$$

The temporal width of solitons is determined by the real positive solutions of the cubic polynomial

$$\varepsilon\eta_{st}^3 - 6\pi\eta_{st}^2 - 3s\varepsilon^2/(8\pi) = 0, \quad (10)$$

and the spatial width is given by Eq. (9). We can thus see that for a stable solution, ν and δ must be of the same sign. This is nothing but a restatement of the well-known fact that stable soliton-type pulses exist only in media characterized by self-focusing nonlinearity with anomalous GVD or self-defocusing nonlinearity with normal GVD. Furthermore, we note that it is not possible to stabilize spatio-temporal solitons with anti-guiding index gradient in a self-defocusing medium since nothing confines the beam spatially.

For clarity of presentation, we focus hereafter only on self-defocusing media with normal GVD and guiding graded index. For this type of medium, we have $\nu = -1$, $\delta = -1$, $s = -1$. For relatively small values of pulse energies ($\varepsilon \ll 1$), we can approximate the stationary state values (Eq. (10)) as $\eta_{st} \approx \varepsilon/(4\pi)$ and $a_{st} \approx 1$. Thus, to lowest order, the temporal width η_{st}^{-1} scales inversely with the energy (or peak power) of the optical pulse, while the spatial width remains constant. Fig. 1 shows the normalized temporal width (solid line) and spatial width (dashed line) of the optical bullet as a function of the normalized energy $\varepsilon \equiv \mathscr{E}_p/\mathscr{E}_0$ [where $\mathscr{E}_0$ is the energy scale defined as $w_0^2 T_0/(k_0 L_d n_2)$]. Whereas the temporal width changes dramatically with input energy, the spatial width changes relatively little.

To examine whether the spatiotemporal soliton is stable, we need to perform a linear stability analysis around the fixed point. Writing $\theta = \theta_{st} + \tilde{\theta}$, $\alpha = \alpha_{st} + \tilde{\alpha}$, $\eta = \eta_{st} + \tilde{\eta}$, and $a = a_{st} + \tilde{a}$, and linearizing in terms of small perturbations from the fixed point, we

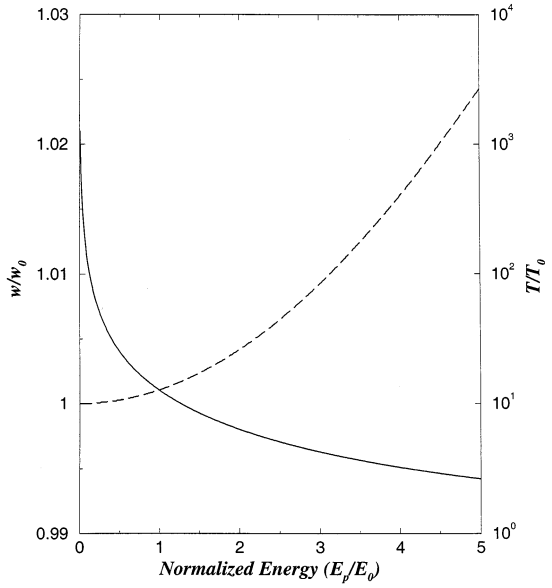

Fig. 1. Normalized temporal (solid line-right axis) and spatial widths (dashed line-left axis) of the spatiotemporal soliton at the fixed point as a function of the normalized energy $\varepsilon \equiv \mathscr{E}_p / \mathscr{E}_0$.

obtain a set of four equations that can be written in a matrix form as

$$\frac{\mathrm{d}}{\mathrm{d}Z}\begin{pmatrix}\tilde{\eta}\\ \tilde{\theta}\\ \tilde{a}\\ \tilde{\alpha}\end{pmatrix} = \begin{pmatrix} F_\eta & F_\theta & F_a & F_\alpha \\ G_\eta & G_\theta & G_a & G_\alpha \\ I_\eta & I_\theta & I_a & I_\alpha \\ J_\eta & J_\theta & J_a & J_\alpha \end{pmatrix}\begin{pmatrix}\tilde{\eta}\\ \tilde{\theta}\\ \tilde{a}\\ \tilde{\alpha}\end{pmatrix}, \tag{11}$$

where the subscripts on F, G, I, and J denote partial derivatives with respect to that variable, evaluated at the stationary state values. The four eigenvalues of the 4×4 stability matrix are given by

$$\lambda = \pm\left(a_{\mathrm{st}} J_a + \eta_{\mathrm{st}} G_\eta \pm \times \sqrt{(a_{\mathrm{st}} J_a + \eta_{\mathrm{st}} J_a)^2 - \left(4 a_{\mathrm{st}} \eta_{\mathrm{st}} J_a G_\eta + \frac{\varepsilon^2 \eta_{\mathrm{st}}^4}{3\pi^4 a_{\mathrm{st}}^6}\right)}\right)^{1/2}. \tag{12}$$

The spatiotemporal soliton will be stable if no value of λ has a positive real part. It is easy to see from Eq. (12) that λ will be purely imaginary if $a_{\mathrm{st}} J_a + \eta_{\mathrm{st}} G_\eta < 0$. Using Eqs. (8) and (10), we find that $a_{\mathrm{st}} J_a + \eta_{\mathrm{st}} G_\eta = -2\eta_{\mathrm{st}}^2[6\pi^2/\varepsilon^2 + 4\eta_{\mathrm{st}}\pi/(3\varepsilon) + \eta_{\mathrm{st}}^2/\pi^2]$ is indeed negative, and the spatiotemporal soliton is stable. Since the real part of λ is zero rather than being negative, the fixed point is neutrally stable in the sense that, in the neighborhood of the fixed point, the soliton parameters will oscillate around the steady-state values. To lowest order in ε, the four eigenvalues are given by

$$\lambda = \pm \mathrm{i}\left(4 + \frac{\varepsilon^2}{2\pi^2}\right)^{1/2} \equiv \pm \mathrm{i} s_1,$$

$$\lambda = \pm \mathrm{i}\frac{\varepsilon^2}{4\sqrt{2}\,\pi^3} \equiv \pm \mathrm{i} s_2. \tag{13}$$

Thus, perturbations around the steady state oscillate at two spatial frequencies s_1 and s_2. These frequencies are quite different for ε as large as 2π. Examination of the eigenvectors shows that the spatial variables (a and α) oscillate at the higher frequency s_1 while the temporal variables (η and θ) oscillate at the lower frequency s_2.

To go beyond the linear stability analysis, we have solved the set (8) of dynamical equations numerically. We plot in Fig. 2 the phase-space trajectories of the dynamical variables. Fig. 2a shows the phase-space trajectories in the η–θ plane while Fig. 2b shows them in the a–α plane. The fixed points are marked by crosses. For small perturbations around the soliton fixed point (upper cross in Fig. 2a), trajectories are nearly circular but become distorted for larger perturbations. The outermost trajectory shows how the system evolves asymptotically towards the CW fixed point (lower cross) for sufficiently large perturbations. However, the spatial width is always bounded because of graded-index waveguiding (Fig. 2b).

The results presented so far are based on the variational method, and one could question the validity of the initial ansatz and the results that are based on it. It is thus necessary to compare the results with a full numerical analysis. To capture the essential physics with manageable computing time, we have suppressed one transverse dimension by setting $Y = 0$ in Eq. (4). The results are, strictly speaking, applicable to planar waveguides but should hold qualitatively even for bulk media. Numerical results show that the spatial and temporal profiles of the soliton do not change when input parameters are close to the fixed point. We have observed such a spatiotemporal

soliton propagating over tens of dispersion lengths which is indicative of the stable nature of the soliton. When input parameters deviate from the fixed point, both spatial and temporal widths oscillate. Fig. 3 shows the root-mean-square (RMS) widths as a function of the propagation distance Z. Although the exact location of the fixed point and the oscillation frequencies are different from those predicted by the variational analysis, the fact that the numerical analysis shows the existence of a stable spatiotemporal soliton is extremely significant. Furthermore, just as the variational methods predicts, the temporal width oscillates on much larger length scales compared with the spatial width. The qualitative agreement between the numerical results and the variational analysis is a strong indication that spatiotemporal solitons exist in a graded-index, self-defocusing, nonlinear medium.

For experimental verification of such solitons, one may use a graded-index fiber whose core is doped

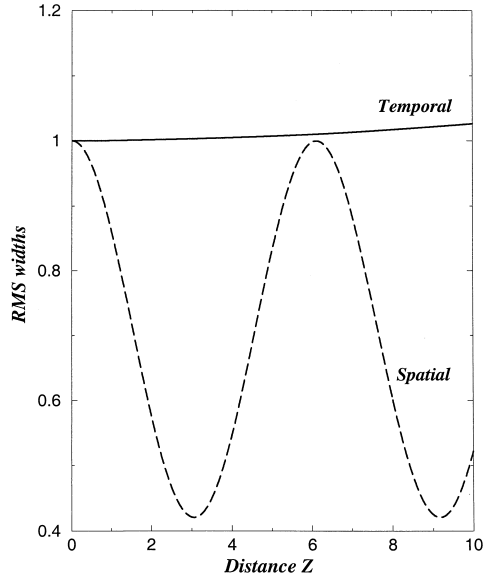

Fig. 3. Normalized temporal (solid line) and spatial (dashed line) widths (RMS values) as a function of propagation distance Z obtained numerically. Values of pulse parameters used are $\varepsilon = 1$, $\eta(0) = 0.1$, $a(0) = 0.9$, $\theta(0) = 0$, $\alpha(0) = 0$.

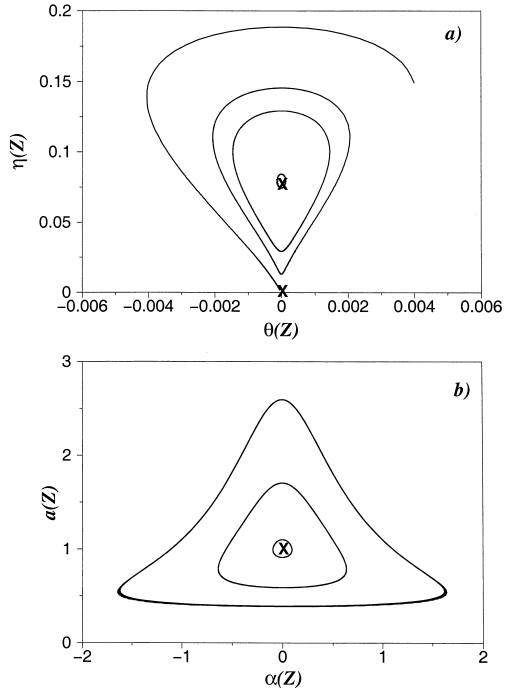

Fig. 2. Phase-space trajectories in the $\eta-\theta$ plane (a) and the $a-\alpha$ plane (b). The fixed points are marked by crosses. In all cases, $\varepsilon = 1$.

with semiconductor nanoparticles. CdS-doped, step-index fibers have been made and their nonlinear properties have been studied [17]. Doping of CdS nanoparticles in a graded-index fiber will provide the ideal material for observing spatiotemporal solitons studied in this paper. To estimate soliton parameters for such fibers, we assume an operating wavelength near 550 nm where $\beta_2 \approx 60$ ps^2/km and n_2 for CdS-doped fibers is negative with a value of about -10^{-16} m^2/W [18]. The parameter n_1 sets the beam-size scale w_0 and can be varied over a wide range. As an example, choose $w_0 = 100$ μm and $n_0 = 1.45$. Then $T_0 \approx 0.1$ ps and $L_d \approx 20$ cm. The energy scale $\mathscr{E}_0 = w_0^2 T_0/(k_0 L_d n_2)$ turns out to be 5 pJ. Such pulses are readily available from modern femtosecond lasers.

Acknowledgements

This research is supported by the National Science Foundation and the TRW Foundation.

References

[1] A. Hasegawa, Y. Kodama, Solitons in Optical Communications, Clarendon Press, Oxford, 1995.
[2] G.P. Agrawal, Nonlinear Fiber Optics, 2nd ed., Academic Press, San Diego, 1995.
[3] N.N. Akhmediev, A. Ankiewicz, Solitons: Nonlinear Pulses and Beams, Chapman and Hall, New York, 1997.
[4] Y. Silberberg, Opt. Lett. 15 (1990) 1282.
[5] M. Desaix, D. Anderson, M. Lisak, J. Opt. Soc. Am. B 8 (1991) 2082.
[6] D.E. Edmundson, R.H. Enns, Opt. Lett. 17 (1992) 586.
[7] X.D. Cao, G.P. Agrawal, C.J. McKinstrie, Phys. Rev. A 49 (1994) 4085.
[8] K. Hayata, H. Higaki, M. Koshiba, Opt. Rev. 2 (1995) 233.
[9] R. McLeod, K. Wagner, S. Blair, Phys. Rev. A 52 (1995) 3254.
[10] W.J. Firth, A. Lord, A.J. Scroggie, Physica Scripta T 67 (1996) 12.
[11] V. Skarka, V.I. Berezhiani, R. Miklaszewski, Phys. Rev. E 56 (1997) 1080.
[12] B.A. Malomed, P. Drummond, H. He, A. Bernston, D. Anderson, M. Lisak, Phys. Rev. B 56 (1997) 4725.
[13] A.W. Snyder, J.D. Mitchell, Opt. Lett. 22 (1997) 16.
[14] X. Liu, L.J. Qian, F.W. Wise, Phys. Rev. Lett. 82 (1999) 4631.
[15] H.S. Eisenberg, Y. Silberberg, Phys. Rev. Lett. 83 (1999) 540.
[16] F. Dalfovo, S. Giorgini, L.P. Pitaevskii, S. Stringari, Rev. Mod. Phys. 71 (1999) 463.
[17] E. Donkor, R. Boncek, SPIE 3075 (1997) 166.
[18] D. Mayweather, M.J.F. Digonnet, R.H. Pantell, IEEE J. Lightwave Tech. 14 (1996) 601.